SUPERCONDUCTORS, METALLURGY OF BETA TUNGSTEN

When discussing technical superconductors one distinguishes between high-temperature superconductors and low-temperature superconductors. The characteristic temperature is the critical temperature, T_c. Above this temperature superconductivity ceases. When thinking about "high" temperatures one typically addresses temperatures around the point of liquification of nitrogen (77 K); when considering "low" temperatures, values in the region of the boiling point of liquid helium (4.2 K) are of interest.

The low-temperature superconductors can be further subdivided. For example, there are solid-solution superconductors and β-tungsten superconductors. In this article, we consider the latter. Another name for β-tungsten superconductors is A-15 superconductors, a classification according to the crystal structure of the material.

Additional main parameters to characterize superconductors are the upper critical magnetic field, B_{c2}, and the critical density, J_c. Again, superconductivity disappears for values of the magnetic field B or the current density J above their critical values.

Solid-solution superconductors, for example, NbTi, are limited to be used up to a magnetic field of about 9 T. Some superconductors of the β-tungsten group have the potential to reach magnetic fields well above 20 T. To take advantage of this potential, many different production methods of wires and tapes have been established. As all A-15 compounds are very brittle, the processing to final dimension takes place in a more ductile state and mainly in combination with substrate materials for electrical and mechanical stabilization. At final dimensions, or even after winding to coils, the superconducting layers are formed during a defined heat treatment.

Many procedures have been developed in order to increase B_{c2} and J_c by adding elements for alloying the basic metals. Because of poor ductility and differences in thermal expan-

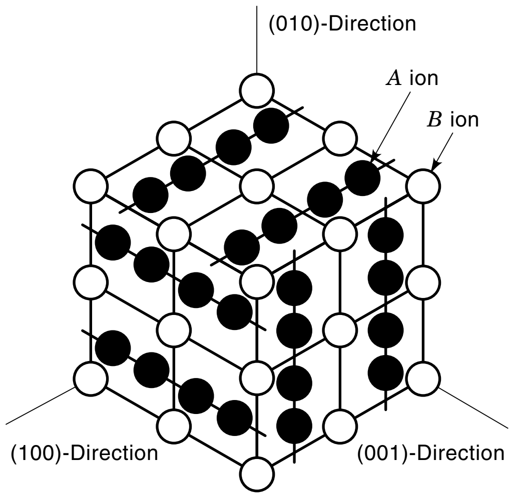

Figure 1. Part of an A15 lattice emphasizing the bcc-sublattice of the A ions and the nonintersecting linear chains of the *B*-ions.

sion coefficients of the materials in such a composite, stress and strain needs to be carefully controlled during handling and in the final application, for example, high-field magnets of different sizes.

This name, used for the class of materials addressed by the title, is based on the β-form of the element tungsten (W), first reported by Hartmann et al. in 1931 (1). This modification is taken as a representant of the A15 structure. As one was not entirely sure whether or not this structure occurs in pure W, but only in connection with oxygen, other prototypes have been sought. The testing of the elements has not been fruitful, and so the lattice of a binary intermetallic compound of chromium (Cr) and silicon (Si), that is, Cr_3Si, became a commonly used indicator. In the following text, the term A15 will be utilized. In the unit cell of a binary compound A_3B, which shows the A15 structure, the ions are ordered in the following manner (see Fig. 1): The *B* ions are arranged in such a way as to build up a body-centered cubic (bcc) sublattice. The *A* ions form nonintersecting chains in the (100)-, (010)-, and (001)-directions on the faces of the unit cell.

In this group of superconductors, however, the *A* ions commonly are niobium (Nb) or vanadium (V), and the *B* ions are, for example, recruited from tin (Sn), aluminum (Al), germanium (Ge), or gallium (Ga), without trying to be exhaustive. Thus, typical representants are materials such as Nb_3Sn, Nb_3Al, Nb_3Ge, or V_3Ga, to name only a few. Other members, together with their transition temperature T_c, can be found in Table 1 (2–4).

The explanation of why a crystal structure is applied in order to characterize a class of superconductors, in spite of the fact that it is not entirely possible to assign superconductivity to a certain combination of qualities, becomes evident noting the following: Until the so-called high T_c superconductors were discovered, the record for the maximum T_c has always been held by members of the A15 family.

All metallic materials being superconducting in the range from 14 K to 23 K have the crystal structure of the A15s. The high superconducting transition temperature T_c for V_3Si and Nb_3Sn has been discovered by Hardy and Hulm (5) in 1953 and Matthias et al. (6) in 1954. A15 materials are expected not to be superconducting above 25 K (7), due to the increasing instability of their structure related to the electron–phonon interaction.

Nevertheless, there are compounds showing the A15 structure which do not have a remarkably high T_c. For example, the intermetallic compound containing Nb and osmium (Os), that is, Nb_3Os, has rather a low one: $T_c = 1$ K (3), whereas the compound of V with cobalt (Co), that is, V_3Co, does not show superconductivity at all, down to a temperature of $T = 0.015$ K (8). That fact made the search for an explanation for the qualities of those materials even more difficult.

In general, it is possible to describe the physical phenomena relevant for the A15s, for example, the high superconducting transition temperature, which is also related to the BCS formula (9), by one-dimensionality, partially localized states near to or at the Fermi level, elastic softness, and strong electron–phonon coupling.

In the A15s, a nonatomic diffusion, characterized by an atomic motion during the transformation at low temperatures, not exceeding the distance of an unit cell's size, takes place. Such martensitic transformations are quite common in solids. The most famous example is an alloy of iron (Fe) and carbon (C), the FeC transformation to the Fe_3C, the bcc-iron or martensite. The martensitic transformation in A15, above T_m (martensitic phase transition temperature) is from cubic A15 to a more tetragonal structure at a few tenths of a kelvin below this temperature. This transformation has been observed first at V_3Si and Nb_3Sn by Batterman and Barrett (10) by x-ray diffraction.

Further investigations have been made by susceptibility and NMR measurement of Knight Shift and nuclear spin lattice relaxation rate (11). Results are that, in the superconducting state, the A15s have the behavior of type-II-superconductors. It is remarkable that, the higher the transition temperature, the higher the temperature dependency of the susceptibility becomes.

The development of technically usable A15s was correlated to the research work done for conductors having a high critical temperature T_c, and being adequate for the production of high-field magnets.

Early progress for commercial use has been achieved with powder metallurgical systems, by filling Nb and Sn powder into a Nb tube, compacting the powder, and drawing the entire piece to the final wire diameter. Other methods targeting the production of tapes, which was possible by passing tapes of the substrate material, for example, V or Nb, through a bath of molten Ga or Sn, respectively. Additional experiments

Table 1. Transition Temperatures [in K] of Some A15 Superconductors (2–4)

A15	Cr_3Si	Mo_3Ir	Nb_3Al	Nb_3Au	Nb_3Ga	Nb_3Ge	Nb_3Sn	Ta_3Sn	Ti_3Ir	V_3Al	V_3Ga	V_3Ge	V_3In	V_3Si
T_c	<1.2	8.5	19.1	11.3	20.7	23.2	18.2	5.8	4.3	9.6	14.8	6	14	17.1

used the same principal approach, by producing pancake-like tapes, made by rolling together already alloyed tapes. Chemical vapor deposition (CVD) and cathodic sputtering are being used, as well.

The advantage of A15 conductors at high T_c and high B_{c2}, the upper critical field (To be precise, the upper critical field would be H_{c2}, which is related to the upper critical flux density B_{c2} in the following way: $B_{c2} = \mu_0 H_{c2}$. But the common combination used in the superconducting society is the one above.) is faced by the disadvantage of the brittle intermetallic A15 compounds. That applies for conductors having reduced mechanical tension in the diffusion layer. In the case of tapes this is given due to the smallness of the distance of the neutral phase to the diffusion layer, resulting in bending stresses low enough to wind magnets after the A15 forming heat treatments.

Tapes, having naturally a large width-to-thickness ratio, are unsuitable for rapidly excited magnets. The A15 layer causes instability because of flux jumps originating from the currents perpendicular to the superconducting layer. Fulfilling the demand of intrinsic stability is one of the important criteria for modern superconducting magnets, and can only be achieved by dividing the superconductive parts into very small portions.

First ideas for the production of fine filaments in a substrate have been laid down in the British patent GB No. 1203292 of 1966 (12). Nevertheless, the advantages of the properties of tapes (Nb_3Sn; V_3Ga) for the design and construction of pancake coil magnets has been used on several high-field magnets. A magnet of 17.5 T (13.5 T with Nb_3Sn plus 4.0 T with V_3Ga), being constructed by Intermagnetics General Corporation (IGC), has been installed at the National Research Institute for Metals (NRIM) in Japan in 1975 (13).

In the case of fine filaments, materials in a ductile state are drawn down to final dimensions. The A15 compound is then formed by a heat treatment, using the solid-state diffusion. This method of solid-state diffusion has first been applied by Tachikawa for a V_3Ga wire (14). The A15 compound is made via a heat treatment at approximately 700°C, which enables the Ga, solved in the Cu, to diffund into the V filaments, forming V_3Ga.

As the problem of brittleness still exists, it has now become common to wind the magnets' coils first, having the treatment afterwards. This so-called wind-and-react method is now used for almost all magnets assembled of A15 superconductors. The structures of V_3Ga and Nb_3Sn are very similar, but material costs and production procedures are in favor of Nb_3Sn. It is possible to perform the solid-state diffusion by several methods. Examples are diffusion of Sn from a bronze with a high tin content into Nb filaments, or by an external diffusion of Sn to a Cu-Nb system with intermediate steps of forming a bronze by the Sn diffusion procedure. The bronze process is applicable, for example, for Nb-Sn, V-Ga, V-Si, V-Ge, Nb-Au, and Nb-Al.

In order to get high critical currents, it is obvious that the reaction of Nb and Sn or V and Ga to Nb_3Sn or V_3Ga must be as complete as possible. Different methods have been developed to reach this target, for example, Nb-Sn internal Sn conductors, powder-in-tube, jelly roll, or in situ technologies. Such methods are necessary, as otherwise the amount of Nb_3Sn in the cross section is limited to the Sn content of the bronze. Compared with conductors produced via the bronze route, these materials are superior, in terms of the critical current density J_c. Forced by design and fabrication technology, those conductors tend to have filament coupling and high hysteresis losses, caused by relatively large effective filament diameters. These values of the effective filament diameters are significantly better for the bronze route conductors, also showing higher figures for T_c and B_{c2}.

Nb_3Al is one of the about 47 known A15 superconductors, having the third highest T_c of 19.1 K (see also Table 1), ranking behind only impractical materials like Nb_3Ge (23 K) and Nb_3Ga (20.3 K). While having those promising figures, the producibility of Nb_3Al turned out to be a difficult task. Different production methods of powder metallurgy have been utilized, as well as the tube and the jelly roll processes.

A15 superconductors are strain sensitive and, while Nb_3Sn may drop about 50% in J_c at a strain of 0.5%, the J_c of Nb_3Al is reduced by 20% only at a strain up to 0.8% (15). That gave reason for renewed interest in that material, especially for large-scale applications like the International Thermonuclear Experimental Reactor (ITER). For the very big coils of such a machine, the conductors are cabled and welded into a stainless-steel conduit, resulting in additional axial strain.

A significant amount of research work has been done toward powder metallurgical solutions, but no commercially usable process has been developed for Nb_3Al. The jelly roll and Nb tube processes seem to be more promising to yield high J_c values at reasonable length. Wires of A15 type superconductors used for the wind-and-react technique need to be insulated with an insulation material like glass, quartz, or ceramic, withstanding the heat-treatment temperature. In the case of Nb_3Sn, this temperature is at approximately 700°C, leading to a braided insulation type of E- or S-glass. The higher temperatures, which are necessary to form the Nb_3Al phase, are another obstacle for a broader use of this material.

While Nb_3Sn became the main choice of the A15 materials being used in a wide section of high-field magnets, a development leading to higher critical currents and better mechanical values is necessary.

The main factor that is limiting high-magnetic field is the Lorentz force, which increases proportionally to the square of the generated magnetic field. The stresses induced into the conductor and the strains require reinforcement, reducing the overall current density and thus leading to magnets being bigger and, therefore, less efficient. The bronze substrate of A15 superconductors is highly resistive and the stabilization is poor. Cu of very good conductivity has to be added [compare Fig. 2(a) with Fig. 2(b)]. Different methods, different with respect to the method of processing the conductors, like internal Sn, jelly roll, and bronze process, are used. In order to prevent the diffusion of B ions, for example, Sn into the Cu, diffusion barriers are necessary. In case of the bronze process conductors, diffusion barriers of Ta or Nb are used.

To influence the superconducting parameters, the critical current density J_c and the upper critical field B_{c2}, by getting better heat-treatment conditions and higher pinning forces, third elements, creating ternary and quarternary alloys, for example, $(Nb, Ta)_3Sn$, $(Nb, Ta, Ti)_3Sn$, or Ge, Hf, or Al are added. As not only J_c but also the overall current, usually denoted by $I_{c,overall}$, is important, the size of conductors has to be increased. This is possible by producing larger monolithic superconductors, mainly of rectangular shape. Another alter-

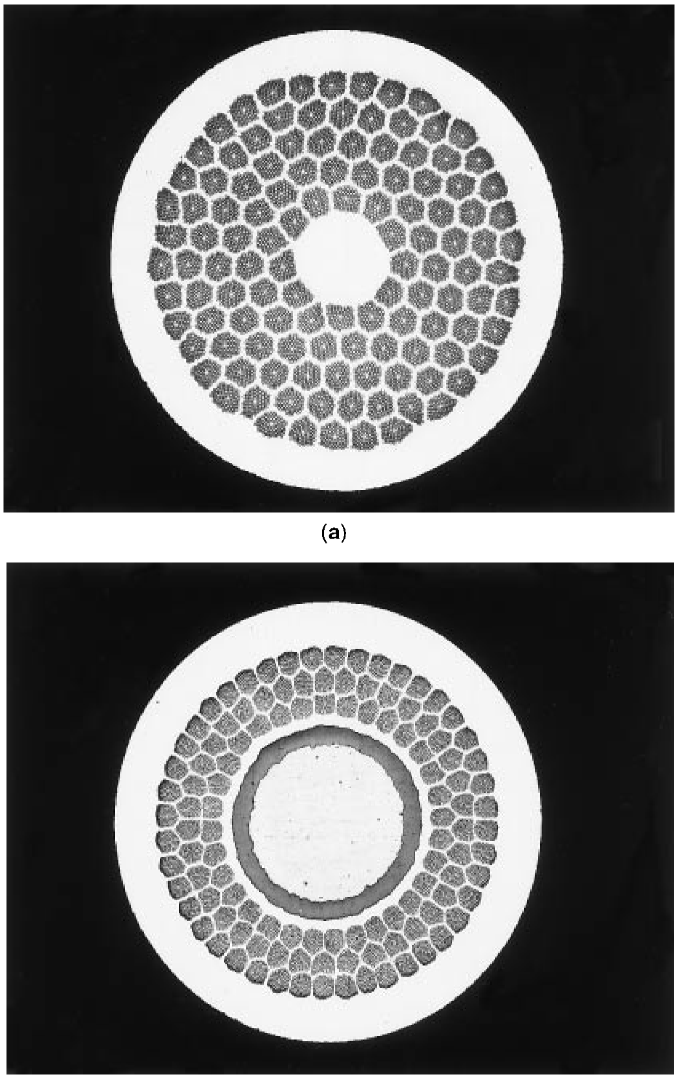

(a)

(b)

Figure 2. Different cross sections of Nb_3Sn bronze conductors; (a) with TaCu core for stabilization; and (b) unstabilized (courtesy of Vacuumschmelze).

native is the cabling of a number of round wires into flat or round cables. Special attention to possible reasons for the reduction of J_c by filament size, the principle conductor design, or the cabling process, has to be given.

To fulfill basic requirements of technically reliable superconductors like high transition temperature T_c, high critical field B_{c2}, and high critical current density J_c, many different approaches have been used. This was mainly done by developing production and material treatment methods adequate to overcome the sometimes difficult material parameters of the A15 components and in order to optimize the parameters of the final conductor configurations. As all A15 materials are brittle by nature, which cannot be overcome by any means, it is necessary to use methods of deformation to get tapes or wires being cold-worked prior to forming the A15 layers. Once the layers are formed, the handling of the conductors needs utmost care, in order not to reduce or completely to destroy the superconducting properties. Deformation of conductors with already existing A15 formation is only possible with complicated, not very practical methods, for example, extremely high hydrostatic pressure.

METHODS OF PRODUCTION

Surface Diffusion Process

In this process, a tape of V or Nb is dipped into a Ga or Sn bath. The heat treatment then forms V_3Ga or Nb_3Sn. It is also possible to hold the bath at the reaction temperature, forming the A15 phase during immersion. To use the better flexibility of tapes and getting the relatively thin layers of the brittle A15 only, other methods, such as sputtering the V or Nb to the core material by cathodic deposition or chemical vapor deposition, or by condensing under high vacuum conditions have been applied. For special MRI magnets, tapes of $(Nb, Zr)_3Sn$ are introduced, operating at 9 K (16).

Composite Diffusion Process

Members of the composite are cold-worked together to final shape. The final heat treatment forms, by solid-state diffusion, the superconducting phase or a microstructure, which also has normal conducting phases. Tapes or even wires made of the components of the superconducting phase, probably in combination with other elements for electrical or mechanical stabilization, or just to improve the workability, are cold-worked together, tapes of Nb and Al or Cu, Sn, and Nb being stacked and rolled. It is also possible to use tapes of the high-melting component with layers of the lower-melting component received by CVD for stacking and rolling. Clad chip extrusion (17), by producing the components as described, chipping and filling them into a Nb-lined Cu can for extrusion and drawing, is another development of this production.

Powder Metallurgy Process

Matrix material like Cu is mixed with other components, for example, Nb and Sn, or Nb and Al, after the compaction to final shape of wires or tapes. The formation of the superconducting phase takes place on the outside of the powder layers. Producing a superconducting wire by PM methods has been approved by Kunzler et al. (18) and was the first successful process for A15 wires. The Nb tube has been filled with (Nb, Sn) powder with a ratio of 3 to 1 or a (Nb_3Sn, Sn) powder. Heat-treatment temperatures of 970°C to 1400°C are used. More recently, powder of the intermetallic compound $NbSn_2$, mixed with Sn powder, is filled into a thin-walled tube of Cu or Cu-based alloy, and reduced in size for compaction. The powder is then placed into a Nb tube within a Cu tube. After that, it is possible to use this combination and stack it again into a Cu can with other matrix parts. Such a billet can be cold-worked to final size without further heat treatment. During the heat treatment, at typically 650°C to 700°C during 15 h to 45 h, a Nb_3Sn layer of about 2.5 μm thickness is formed on the inner side of the Nb tube, resulting in filament diameters of 10 μm to 20 μm, depending on the number of cores. The reaction process is, in fact, a two-step process of $NbSn_2 + Sn \rightarrow Nb_6Sn_5$ from the core, and then forming with the Nb tube and, by depleting, of Sn the Nb_3Sn. Similar methods can be used for Nb_3Al, especially by using sintered rods of Nb powder, metal-impregnated to get it self-supporting,

Table 2. Increase of Hardness of Niobium and Tin Bronze During Deformation (20)

Sample	Degree of Deformation (%)	Heat-Treatment Time (h)	Temperature (°C)	Hardness (N/mm^2)
7.7 at. % Sn	0	—	—	1260
	21	—	—	2230
	27	—	—	2330
	21	1	500	1340
	21	5	500	1160
	21	8	500	1140
8.5 at. % Sn	0	—	—	1350
	21	—	—	2560
	21	1	400	1640
	21	5	400	1370
	21	8	400	1330
Nb, original	0	—	—	1020
Nb Core	25	—	—	1330
	57	—	—	1480
	68	—	—	1460
	75	1	550	1530
	97	1	550	1510
	99.7	1	550	2030

due to immersion into Al-Ge or Al-Si baths at temperatures of 600°C or 580°C, respectively (19). Reaction treatment at 1700°C is followed by final annealing, at 750°C.

Bronze Process

This technology is very typical for Nb_3Sn and V_3Ga superconductors. In a substrate of Cu-Sn or Cu-Ga, a number of filaments of Nb or V are inserted. The solubility of Sn and Ga is limited to approximately 8 at.% or 20 at.%, respectively. This solubility restrains the amount of the A15 compound that can be formed by solid-state diffusion. The high-strength component, the bronze, is getting the low-strength component, Nb-Ga, to a laminated flow, but multiple intermediate heat treatments due to work hardening are necessary; see, for example, Table 2 (20). Relatively thin filaments, with a maximum diameter of about 5 μm, are necessary to receive good overall current density. The Sn reservoir and the diffusion path is the bronze between the filaments, but the decreasing content of Sn during the reaction treatment reduces the speed of diffusion. Heat treatments at about 700°C, in many different variations, form the intermetallic A15 compound at the interlayer of the bronze to Nb or V. This also creates Kirkendall voids (21), which disturb the diffusion paths; see Fig. 8. To get high filament numbers for conductors of bigger size and due to the limitations in filament diameter, second and third stacking of billets may be necessary. For electrical stabilization, Cu can be embedded in the matrix or in the center of the conductor. An outer shell of Cu is also possible, especially in the case where a larger amount of Cu is needed; see Fig. 3. Diffusion barriers of Ta, Nb, or V are necessary, to protect the Cu during the diffusion process by preventing *B* ions entering from the bronze into the Cu, which would significantly reduce the conductivity.

Internal Sn Process

A Cu jacket, having a Sn rod in the center and Nb cores distributed around it in the remaining cross section, is the starting element of this process. Those subelements may be surrounded by Nb or Ta barriers, to protect the stabilizing Cu from diffusion of the Sn. This Cu is the outer tube into which the subelements are inserted. The Cu-Nb-Sn composite is cold-worked to final dimension, without intermediate annealing. The bronze matrix is formed when the conductor already is in its final shape. Therefore, the heat treatment needs two cycles. The first typically starts at 200°C for 100 h, continues at 375°C for 24 h, and finishes at 580°C for 50 h. It is needed for the homogenization of the Cu-Sn bronze, containing different phases according to the phase diagram in Fig. 4 (23). A consecutive second heat treatment of one or more steps is necessary to form the Nb_3Sn layer. The typical temperature is around 725°C. For a better distribution of the Sn, methods of placing it rather close to the filaments instead, as a core in the center of the subelements, is used, resulting in reduced heat-treatment time and a homogeneous A15 layer distribution over the cross section of the conductor (24).

In Situ Process

Casting ingots of two-phase Cu-Nb or Cu-V with dendrites dispersed into the matrix of Cu, cold-working, and then coating with Sn or Ga, are the basic steps to start this process [Fig. 5(a)]. To reduce the likelihood of wire-breakage, a bronze matrix may be used. After dispersing the Sn or Ga throughout the matrix, Nb_3Sn or V_3Ga are formed during the heat treatment at the interfaces between the matrix and the filaments. Highly homogeneous Cu-V ingots are difficult to produce by conventional casting methods, due to a large miscibility gap in the liquid region. A continuous arc casting plus Ga coating give the opportunity to optimize the material toward better mechanical values and better current-carrying capacity. Large ingots up to 150 mm in diameter [Fig. 5(b)] have been produced by smelting the Cu-Nb into a CaO mold for solidification. Wires produced thereof have shown, after heat treatment at 800°C for 25 h, good mechanical values in untwisted condition. No degradation is found up to 1.2% strain, but in

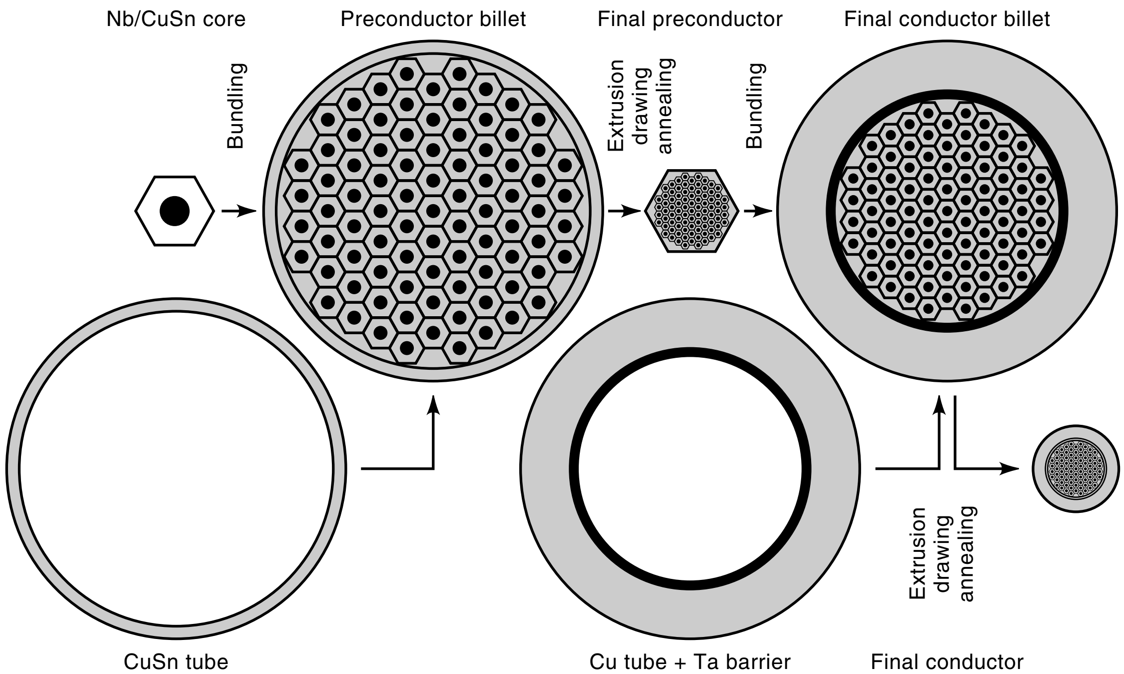

Figure 3. Fabrication of bronze route conductors (courtesy of Vacuumschmelze).

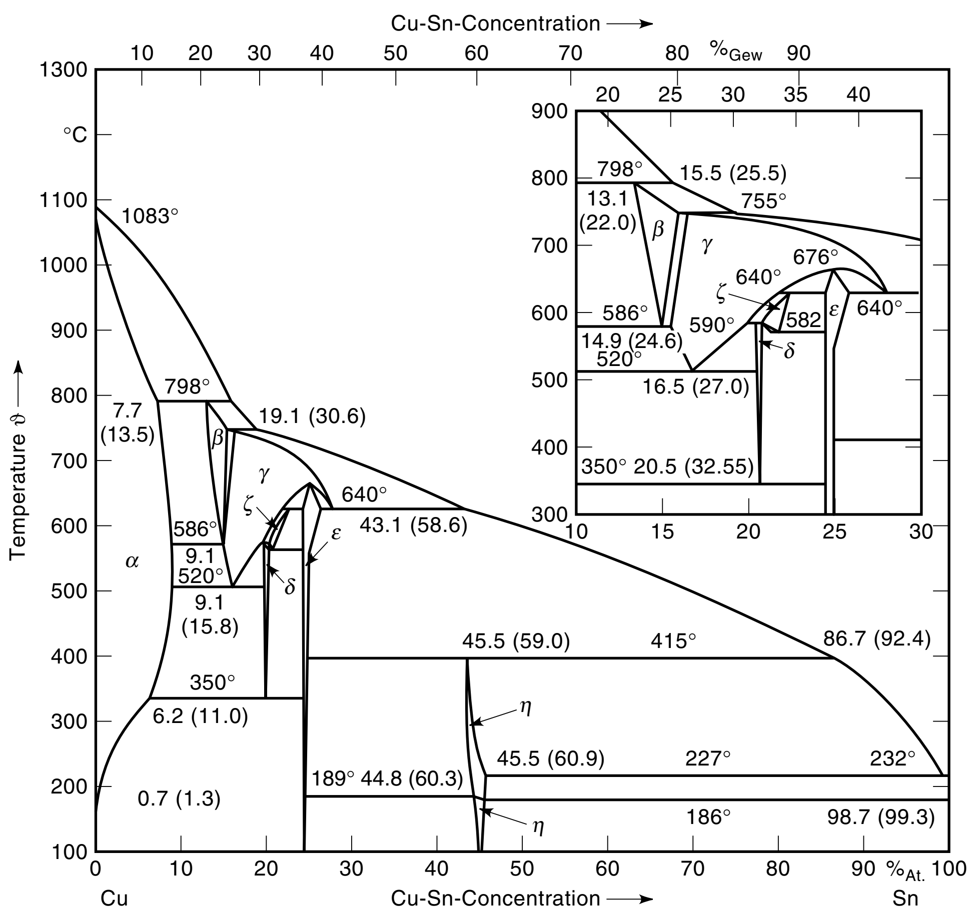

Figure 4. Detailed phase diagram of Cu-Sn (23).

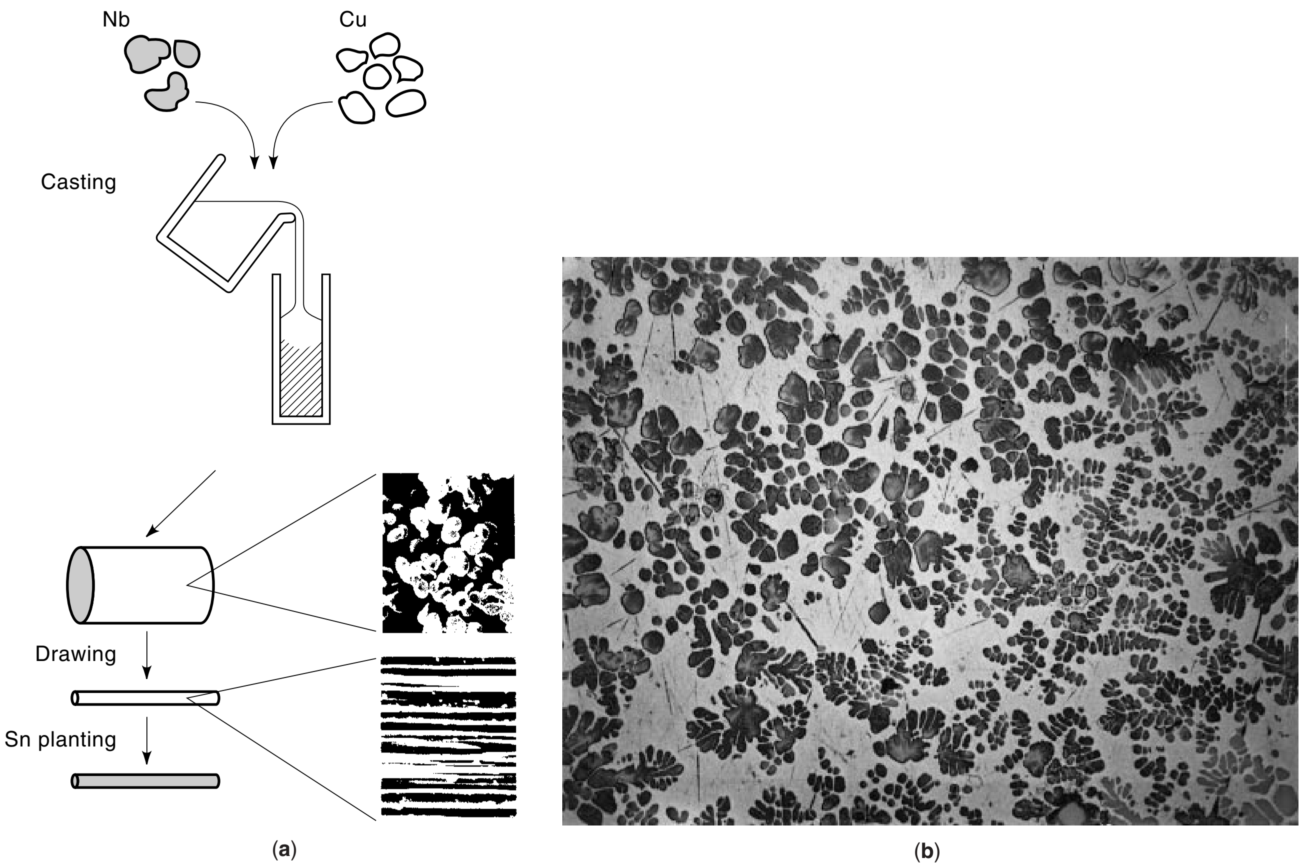

Figure 5. (a) Schematic diagram of in situ process of Cu-Nb composite (courtesy of Fujikura). (b) Transverse section showing Nb dendrite solidified in Cu mold (courtesy of Fujikura).

the case of twisted wires, the degradation is significant (25a). Multistage cables made from fine wires with a diameter of 0.2 mm with small in situ filaments of 0.5 μm have been developed for ac applications. Such cables are showing even more improved values in strain resistance (25b).

External Diffusion Process

This process is also typically used for V_3Ga and Nb_3Sn composites. In a Cu billet with drilled holes, rods of V or Nb are embedded and cold work is applied to get the final dimensions. Prior to heat treatment, the surface is coated with Ga or Sn having first the diffusion into the matrix, and then forms at the interface between matrix and the cores the V_3Ga or Nb_3Sn layers, respectively. The amount of A15 phase produced by this method is limited by the quantity of the B material which can be stored in the coating of the Cu-A wire. This fact dictates the maximum diameter of the wire. The combination of this method with the bronze process, in order to increase the tin content, is also possible.

Jelly Roll Process

A foil of Nb with slit meshes and a foil of Cu-Sn bronze are spirally rolled into a cylinder, cold-worked, and heat-treated. The Nb_3Sn is received at the interface of the Cu-Sn and the Nb. Despite the successful use of the jelly roll process for the Nb_3Sn, this method was originally developed for Nb_3Al (26). Foils of Nb and Al have been wrapped around one Cu cylinder and inserted into another Cu cylinder. Wires with a diameter of 0.2 mm receive a heat treatment of several hours at about 850°C, resulting in a mixture of Nb_3Al and nonreacted Nb. Placing some, for example, nine, of the unreacted jelly rolls into a Cu rod with drilled bores, is a logical way to increase the current by getting a larger cross section. The modified jelly roll technology is performed (27) by wrapping layers of Cu sheets and expanded metal sheets of Nb around a Sn rod. Conductor designs with 54 of such jelly rolls assembled with a barrier of Nb or V are placed in a Cu can for cold-working to final dimensions, providing a high J_c and large Cu cross-section, likewise. In principal, the modified jelly roll process proceeds like the internal Sn process.

Tube Process

To form the basic composite, a Cu tube with a Sn or Cu-Sn alloy core is inserted into a Nb tube. This combination is introduced into another Cu tube and then cold-drawn. A number of those single-core elements are stacked for assembling into a Cu can and cold-worked to final dimension. For the production of basic composites of larger conductors, cold working is performed down only to intermediate dimensions, followed by a second assembly. During heat treatment, the Sn diffusion into the matrix takes place first. Then the Nb_3Sn layer is formed at the interface of the Cu to the inner side of the Nb tubes. This technology has also been used for V_3Ga wires and tapes, rolled from wires (28).

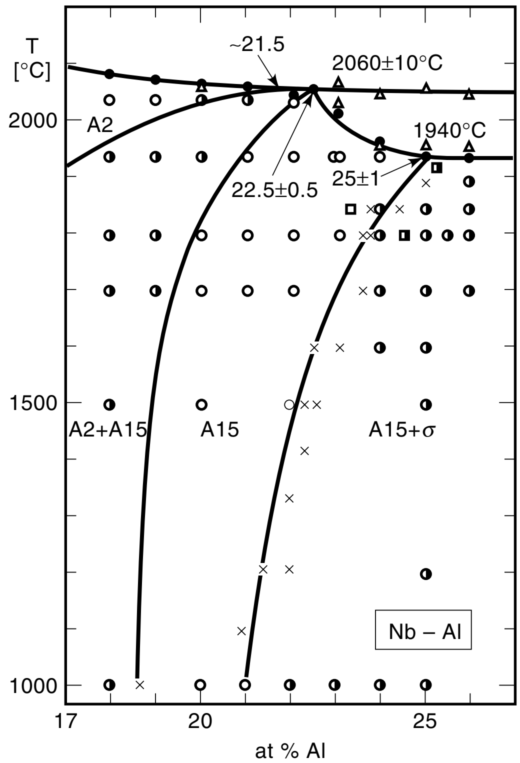

Figure 6. Detailed phase diagram Nb-Al (29).

Specialties of the Production of Nb_3Al

The A15 phase in Nb_3Al can be attained from the melting bath using high temperatures, and at reduced temperatures for the reaction between Nb and Nb_2Al. The σ-phase of Nb_2Al needs temperatures above 1600°C. By reacting with Nb at about 1800°C, A15 is formed. The desired stoichiometry of the A15 phase seems to be stable at high temperatures of ≥1770°C only (1940°C in the corner of the phase diagram of Fig. 6 (29). In general, the high reaction temperature for the conventionally processed materials leads to grain growth. Because many production techniques failed to get stoichiometric Nb_3Al, numbers of different approaches have been tried, like laser alloying or rapid quenching by melt spinning. Powder metallurgical processes are unfavorable, because of the high oxygen (O) content in the powder, which does not allow the high deformation rate required. To get reliable conductor lengths, especially for magnets with magnetic fields above 21 T, a distinct rapid-quench process has been established (30). By the jelly roll technology, the wire consisting of several elements made from Nb and Al sheets wrapped around an Nb core is produced, using multistacking and extrusion procedures, resulting in a cross-section pattern, as can be seen in Fig. 7. The wire produced this way is subject to ohmic heating at 1900°C to 2000°C, and rapidly but continuously quenched in a bath of molten Ga (melting point: 30°C); see Fig. 8. Such a treatment leads to a supersaturated Nb-Al-bcc phase. This metastable phase is transformed by a heat treatment of 700°C to 900°C to microcrystalline A15 of nearly stoichiometric composition. The resistivity ratio RRR in the Nb matrix has a value of about 17, giving reduced concern about bridging of filaments in this kind of conductor. Due to the processing, the wire consists of Nb-Al only, with access of Nb. For the use at a higher current J, Cu has to be clad, in order to stabilize the wires.

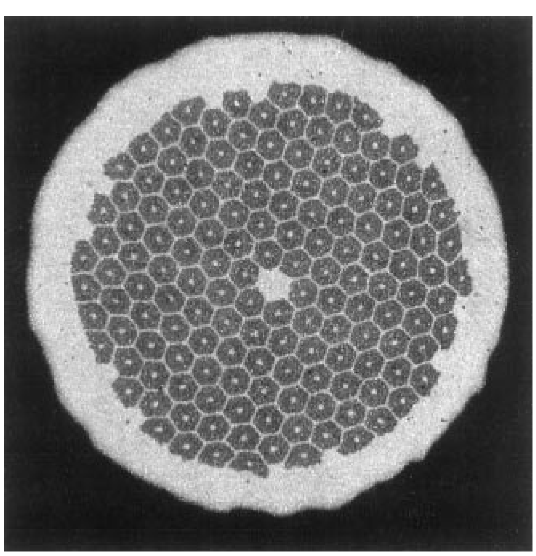

Figure 7. Cross section of Nb/Al composite wire (30).

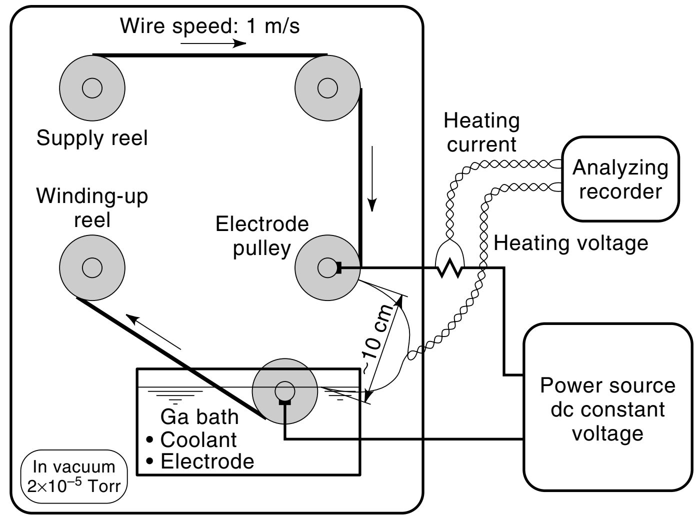

Figure 8. Schematic diagram of rapid-heating/rapid-quenching apparatus (30).

BRONZE CONDUCTORS

To fabricate high-field magnets, flexible tapes, having the advantage of a small distance from the brittle A15 compound to the neutral phase in bending direction, have been used successfully. The large area-to-thickness ratio of the A15 layer leads to instability (flux jumps), especially if magnets have a rapid ramping rate. The solid-state diffusion process, as used for bronze conductors of Nb_3Sn and V_3Ga (31), has solved this problem, by dividing the core material into plenty of fine filaments. The formation of A15 layers is principally limited by the amount of Sn and Ga in the bronze. The solubility of Sn in Cu is 8.5 at.% and for Ga in Cu is 20 at.%. Bronze with about 7.5 at.% Sn or about 18 at.% Ga has been used. The

Table 3. Maximum Area Ratio, Remaining Tin Concentration, and Transition Temperature of Solid-State-Diffused Nb_3Sn Samples (20)

Tin Concentration in Alloy (at. %)	Diffusion Temperature (°C)	Maximum Area Ratio $A_{Nb_3Sn}/A_{Cu(Sn)}$	Remaining Tin Concentration (at. % (calculated)]	Transition Temperature T_c(K)
7.7	700	0.15	5.1	17.5[a]
	730	0.18	4.6	
	750	0.26	3.3	18.1[b]
8.5	750	0.30	3.4	18.04[b]

[a] Heat-treatment time: 24 h.
[b] Heat-treatment time: 66 h.

diffusion process forms the A15 layer until the equilibrium for a given temperature is established. At a temperature of 620°C to 700°C, the diffusion for Ga ends at a remaining concentration at 14 at.% to 15 at.% Ga in the matrix. Sn diffusion from the bronze proceeds at approximately 700°C to 850°C, leaving a Sn concentration in the bronze of approximately 3 at.% to 4 at.%; see Table 3.

The heat-treatment time and temperature has to be controlled in such a way as to receive an optimum layer thickness, but without increasing too much the grain size. Especially for a long heat treatment of ≥200 h, the matrix volume has to be increased, in order to provide enough Sn or Ga. Small distances between the filaments seem to be desirable, due to reduced bending strain, but the space between the filaments acts as a diffusion path for the B ions from the conductor periphery, too. Those diffusion paths are reduced in their effective width by the Kirkendall voids (see Fig. 9) (32) caused by the diffusion mechanism during heat treatment. At a given temperature and a constant concentration gap, the quantity of B ions diffusing through a cross section in a given time is proportional to the area of this cross section (Fick's first law). From this follows that the cross section of the cores of Nb or V should be divided in as many portions as feasible, to increase the interlayer between the bronze and the core material. This leads to an increase of the total amount of A15 material, even with reduced heat treatment time. Optimization studies of diffusion treatment versus layer thickness have shown that filament diameters should be in the range of 3 μm to 5 μm. For conductors with a diameter of 1.5 mm, and taking into account the cross section needed for stabilization and diffusion barrier, approximately 15,000 filaments are necessary. Workability of the component is an essential request to arrive with technically and commercially usable conductors. While the basic components, Nb or V, electron beam- or arc-melted, are high-purity materials of excellent ductility, they are sensitive to imbrittlement by interstitials of oxygen (O), nitrogen (N), or C. This is especially true for the V, but the more problematic part is the bronze; see Table 2. Normally Cu-Sn bronze contains about 10 wt.% Sn, and as desoxidizer phosphorus (P) is used. In the Nb-Sn system, P prevents the diffusion procedure. The amount of Sn should be as close as possible to the solubility limit of 8.5 at.%. For many years, the technically attainable Sn content was limited to about 8 at.%. Newer processes made homogeneous bronze at 8.5 at.% Sn available (33). The positive influence of the Sn content on J_c is shown in Fig. 10. During cold work, the hardness of the bronze is increasing rapidly, as shown in Table 2, and a significant number of intermediate heat treatments have to be applied. From the workability point of view, this is certainly a disadvantage of the bronze process.

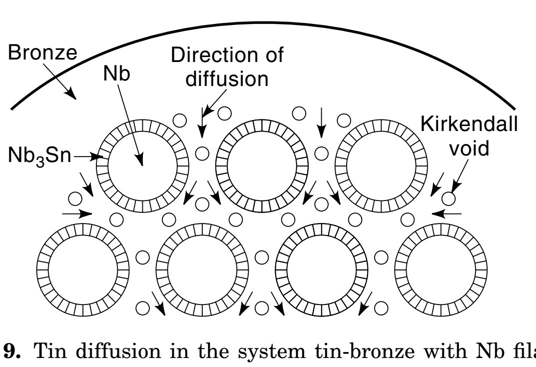

Figure 9. Tin diffusion in the system tin-bronze with Nb filaments showing the narrowing of the diffusion paths by the Kirkendall voids; after (32).

STABILIZATION AND BARRIERS

To have maximum J_c, the core material has to be converted into A15, theoretically to 100%. Regarding mechanical and electrical stability, a small core of unreacted material, even in fine filaments, has a positive influence on the overall per-

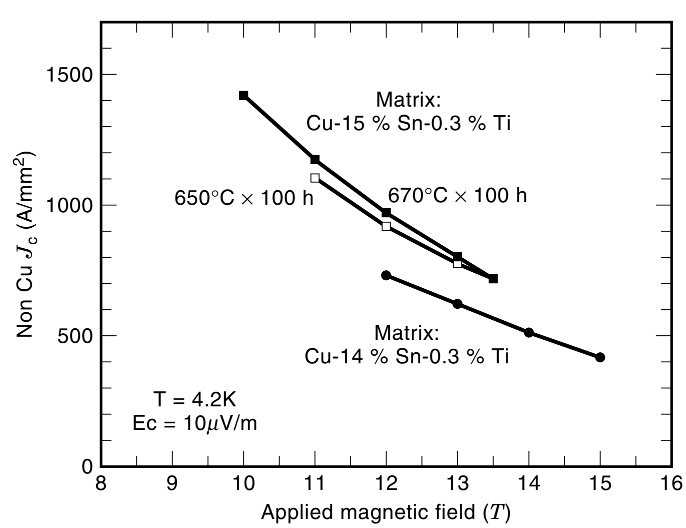

Figure 10. Diagram of non-Cu J_c versus applied magnetic field H showing the enhancement of J_c by the Sn concentration (30).

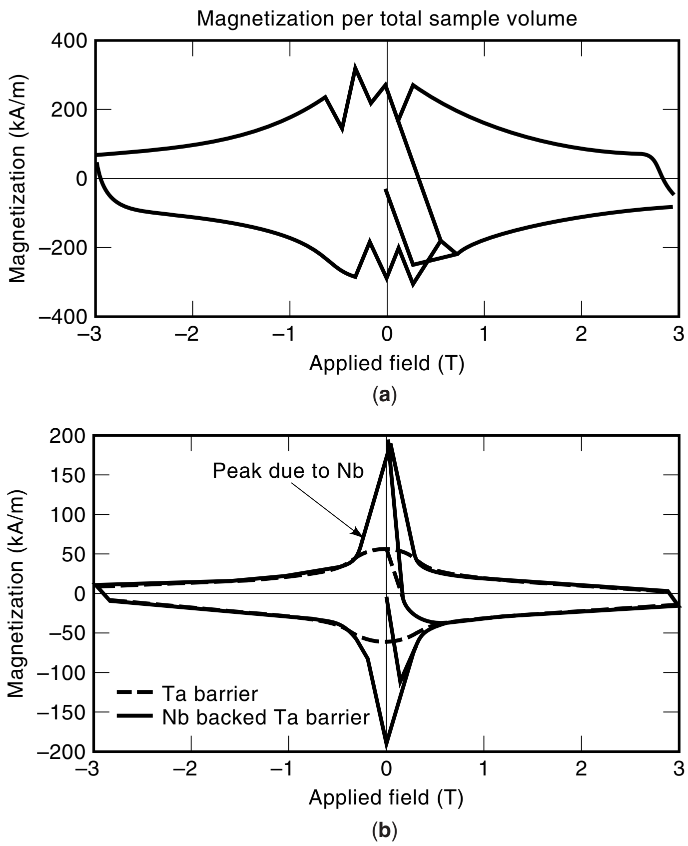

Figure 11. Magnetization curve for material; (a) containing a 100% Nb barrier: The relatively large flux jumps in the low field region are very apparent; and (b) containing an interrupted Nb barrier: No flux jumps in the low field region are observed (24).

formance of the conductor. For reasons of electrical and thermal stabilization, for example, during the occurrence of a quench, which may result from wire movement in connection with energy dissipation, it is necessary to have a highly conductive material in the cross section. The bronze itself has a rather low conductivity (specific resistance $\approx$ 70 nΩm at a temperature of 4 K), which is important to reduce the alternating current (ac) losses. Experiments have shown that, in case of bronze conductors, a reversed transport reaction can lead to a very small (0.3 at.%) Sn content, compared with the values of Table 3. In this low-Sn "bronze," the value for the specific resistivity is reduced by a factor of 10. This method is not very practical and has, in view of ac losses, disadvantages. It is therefore necessary to increase the electrical stability by designing conductors with Cu included in the cross section. This can be done by a few percent distributed throughout the matrix, up to 20% in the wire center and up to a maximum part of the cross section as an outer shell. The composite needs a barrier to protect the Cu from the diffusion of B ions into the stabilizing part, which would reduce the conductivity of the Cu. Barrier materials fulfilling this task are V, Nb, Ta, or alloys and combinations thereof (34). The use of a Nb barrier seems to be the natural choice, as it fits the material parameters of the complete conductor. The Nb_3Sn layer formed at the interface of bronze and barrier acts just like a large filament, bringing additional high ac losses. The effect of the barrier materials on the hysteresis losses is shown in Fig. 11(a) and Fig. 11(b). The use of Ta barriers avoids magnetic disturbances, even in cases where high-temperature heat treatments are being used. Furthermore, Ta barriers are effective as reinforcement due to their high Young's modulus and remarkably high strength at 4 K. Access of O must be prevented during any heat treatment in the course of production and the diffusion procedure, as Ta interacts intensively with O. Conductors with peripheral stabilization should have $\geq$25% (area) of Cu, in order not to get a Cu layer $\leq$10 μm, as O might penetrate into the Ta (32). Barriers of Ta penetrated by O are likely to burst during the final diffusion treatment. Further solutions might be the use of a Ta core, increasing the yield strength significantly by the larger cross section of Ta. Enlarging the Ta portion of the cross-section area to $\geq$10% results in yield strength $R_{p0.2}$ of >250 MPa. See Fig. 12(a) and Fig. 12(b) (35) for the characteristics and the cross section of a high-yield-strength conductor.

Al may act as a stabilizing material due to its attractive properties: low weight, high specific residual resistivity ratio RRR (>1000), high thermal conductivity, and low magnetoresistance. For practical, use, restrictions arise from the poor mechanical values, not compatible with the other components of bronze conductors. The melting point of Al is lower than the reaction temperature. Thus, Al is only useable for reacted conductors, giving the need for the react-and-wind technology, which does not implement too high a strain in the conductor during winding, but which is feasible for large magnets only. Monolithic and cable conductors can be coextruded together with high-purity Al and reinforcing elements of special steel or cobalt-(Co)-based alloys (36). In case a high overall current I_c is needed, electrical stabilization is possible by cabling of unstabilized or stabilized wires together with Cu wires. It is essential that those Cu wires are also protected by diffusion barriers, which must have an outer Cu or Cu-Sn layer to avoid O penetration into the Ta. An example of a cable with additional stabilizing CuTaCu wires is shown in Fig. 13. Prereacted cables, soft-soldered to Cu clad tapes of Al, have been used for special laboratory magnets. To build very large coils, as necessary for Tokamak fusion technology like ITER, conductors with critical currents of about 100 kA at 12 T and excellent mechanical values are needed. The present way to fulfill such demands is to produce a round cable of many superconducting wires (ITER: >1000 wires) in a multicabling process, embedded into a stainless-steel jacket. By this method, good cooling conditions are received as well.

A direct relationship exists between J_c and ac losses: With increasing J_c the ac losses are increasing as well. The most important reason for such losses in internal-Sn and jelly roll conductors is filament bridging during the reaction treatment and barrier material like Nb. The increase in volume caused by the diffusion of Sn is about 30% to 40% in the Nb_3Sn layer, while the outer wire dimension is practically unaffected. The filament bridging results in huge effective filament sizes d^*. In powder-in-tube conductors, the filament size depends on the grain size of the $NbSn_2$ powder. As the forming of the Nb_3Sn layer in the tube process takes place at the interface between the Cu and Nb tubes, large filaments are received. Barriers of Nb behave like large filaments, too. Bronze-processed conductors have the lowest ac losses and smallest d^*, as bridging in the bronze matrix is negligible. Bridging is also not a problem for Nb_3Al conductors. The filament diameter of conductors produced by the jelly roll technique is in the range of 50 μm. The specification of the ITER conductors is, in re-

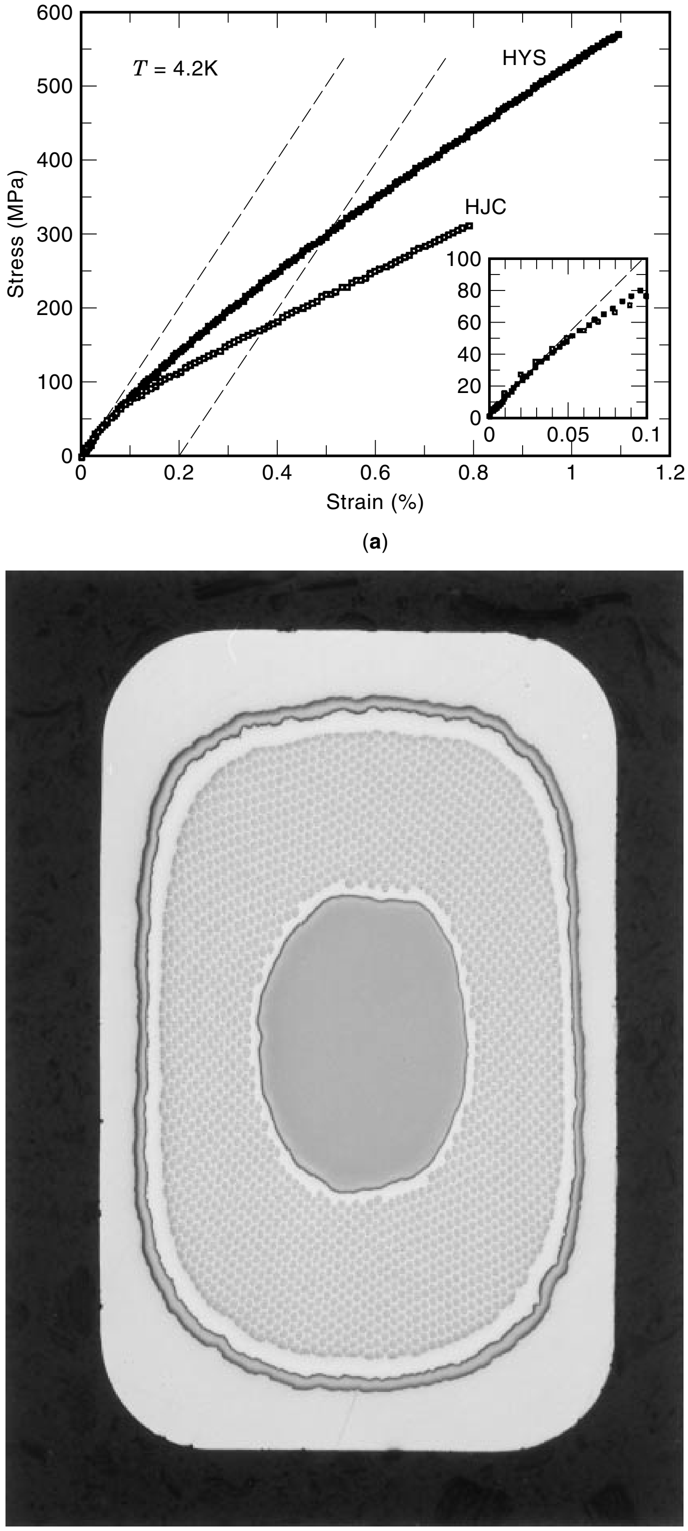

Figure 12. Stress/strain characteristics at a temperature of 4.2 K of a high yield strength conductor compared with a high-J_c conductor (35) and cross section of the high yield strength conductor with a Ta core (courtesy of Kobe Steel).

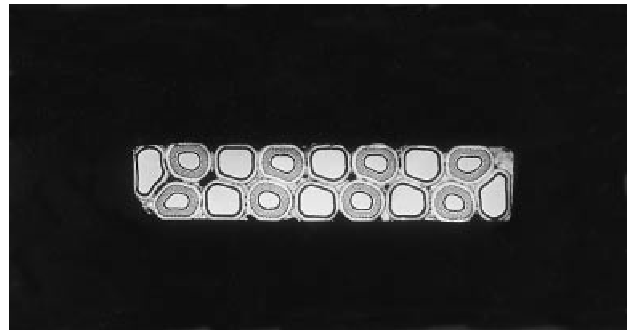

Figure 13. Superconducting cable consisting of eight bronze conductors with a TaCu core and eight additional stabilizing wires of Cu-TaCu (courtesy of Vacuumschmelze).

gard to this fact, divided into two parts—one of high J_c and high ac losses (HP I), and the other with a low J_c and low ac losses (HP II); see Table 4. A reduction of ac losses in internal-Sn conductors is possible, by reducing the Sn content, but matching the properties of a bronze process conductor, like the one shown in Fig. 14(a) will be hardly possible, see Fig. 14(b).

Degradation by Cabling

The selection of the jacket material has to take into account that almost no additional strain should be induced into the conductor by the properties of the conduit. The critical current of A15 superconductors is depending on the stress strain conditions. It is also necessary to consider the behavior of the conduit material during the heat-treatment cycles (react-and-wind) applied for reaction. While cabling seems to be a logical approach to increase the current-carrying capacity, degradation during this process may happen, especially for Rutherford type, flat cables. The sensitivity to the deformation which takes place at the edges of flat cables is in dependence to the conductor design and making. Bronze conductors, with and without stabilization, exhibit a degradation of only 5% and, even as specially enhanced designs, not more than about 10%. Other configurations like internal-Sn have shown a significantly higher degradation of the critical current J_c (37). Generally, cables of A15 are workable with bronze conductors or with powder-in-tube conductors. In the case where cables made from Nb_3Al wires of the continuous-quench method are applicable, internal-Sn conductors have potential for improvement (24). Jelly roll conductors of Nb_3Sn exhibit high sensitivity to strain-induced damage and are thus not suitable (38). For cables consisting of many single superconductor wires, sintering of the wires during heat treatment has to be avoided, and coupling losses must be reduced by the resistance between them. Cr plating of about 2 μm thickness appears to be suitable to fulfill those topics. Problems with the RRR of the stabilizing Cu may arise, due to the heat treatment. Thus measures have to be taken against this effect.

The Cu content of modified jelly roll and internal-Sn conductors is, in the basic design, larger than that of the bronze conductors. Due to the high Sn content in these composites, the J_c, in particular, the non-Cu J_c, taking into account the cross-section area without stabilizing portions, is superior as well. The Cu content can be varied up to above 60% (area). However, a minimum of about 30% is needed, in order to have

Table 4. ITER Strands: Test Results and Specifications (38)

Technique	Bronze	Bronze	Internal Tin	Internal Tin	Internal Tin	HP I (spec.)	HP II (spec.)
Diameter (excluding Cr-layer) (mm)	0.803	0.802	0.801	0.806	0.802	0.81	0.81
Barrier	Ta	Ta	Ta	Ta + Nb	Ta/Nb		
Thickness barrier (μm)	10–15	6–8	5	1 + 2 − 3	3		
Twist pitch (mm)	8.8	18.4	18.0	9.9	9.3	≤10	≤10
Heat-treatment temperature and time (°C/h)	570/220 650/175	650/240	200/6 350/18 450/28 580/180 650/240	220/175 340/96 650/180	185/120 340/72 650/200		
Filament reacted	partially	partially	fully	fully	partially		
Cu/non-Cu ratio	1.49	1.49	1.59	1.38	1.61		
Critical temperature T^* at 13 T (K)	10.2	10.2	9.31	9.49	9.31		
Upper critical field $B_{c2}{}^*$ (T)	28.3	27.7	24.9	25.3	24.6		
Cr thickness (μm)	2.1	3.2	2.6	1.7	2.3	2	2
RRR (resistivity at 273 K/resistivity at 20 K)	150	147	130	80	213	>100	>100
Overall strand density (g/cm^3)	9.33	9.14	9.04	8.98	9.01		
Non-Cu J_c at 12 T, 4.2 K, 0.1 μV/cm (A/mm^2)	550	570	780	710	680	>700	>500
Non-Cu hysteresis losses, 3 T cycle at 4.2 K (mJ/cm^3)	94	91	136	595	599	<600	<200
n value at 12 T, 4.2 K, 0.1 μV/cm						>20	>20
Coupling loss time constant (ms)	0.62	3.1	1.3	5.9	6.3		

an outer Cu shell, which is necessary for mechanical stability during processing.

Stress and Strain

The mismatch of thermal expansion coefficients of the conductor components is creating compressive strain in the A15 layer during cooling. The difference from the heat-treatment temperature to 4.2 K is approximately 1000 K. The influence of strain on the I_c, values was presented first by Buehler and Levingstein in 1965 (39). The compressive strain influences the T_c and B_{c2} values as well. The relative difference in linear expansion, $\Delta l/l$, of separated bronze and Nb_3Sn for ΔT of 1000 K, is about 1.05% (32). Depending on the volume-ratio of Nb_3Sn to the bronze and for a conductor that has good bonding between its elements, the contraction is between 0.00% and 1.05%. This is because the filaments are under tensile stress and the bronze are under compressive stress. Measurements on Nb_3Sn with removed bronze matrix show a T_c close to the maximum 18.2 K. The values for prestressed conductors are reduced by about 1 K. Conductor designs which have besides the matrix and the twisted filaments, stabilizing Cu, diffusion barrier, or reinforcing components, for example, Cu-Nb, are a rather complicated system. For example, regard the following values: A conductor with 22% (area) Cu and 5% Ta has a relative thermal contraction from room temperature down to 4 K of −0.29%, whereas conductors with 33% Cu and 10% Ta have −0.26%.)

The critical values decrease by the compression but increase again under axial tension. Maximum I_c is gained at the strain ϵ_m, where the tensile force in the filament is reduced to a minimum. The Young's modulus in the filament area is in the range of 130 GPa and for the bronze between 50 GPa to 80 GPa (40). The value for the bronze depends on the depletion of the Sn. By the diffusion process the Sn content is reduced and Kirkendall voids are created. These effects, the high temperature for annealing and the length of the heat treatment influencing the grain structure, are responsible for a low yield strength in the bronze. Plastic deformation of the bronze caused by tensile stress, due to mismatch of the thermal expansion coefficients (bronze: 16×10^{-6} K^{-1}; Nb/Nb_3Sn: 7×10^{-6} K^{-1}), results in reduced differences in the thermal contraction. Bare Nb_3Sn shows breaks at strain of about 0.2%. Prior to breaking, slip-steps with an angle of 45° can be observed. The precompression built up in the conductor has, as a consequence, the drop of I_c, B_{c2}, and T_c. The same precompression acts as a mechanical reserve during elongation of the conductor, though strain of 0.7% to 0.8% is possible for the complete composite without irreversible I_c degradation (32). This decreasing under compression and increasing under tension is reversible, as long as a critical strain in the filament was not exceeded. If strain was too high, I_c would not recover completely after the load was released, because of cracks in the filaments; see Fig. 15.

The increased strain tolerance is an important reason for the fact that bronze conductors can be used as technical superconducting wires. Consequently, a thicker layer of Nb_3Sn leaves a more Sn-depleted bronze with reduced Young's modulus. Possible plastic deformation and the reduced Young's modulus are diminishing the compressive strain of the filaments and, therefore, the degradation of the critical values is smaller. The mechanical reserve against axial stress is smaller, too. The filaments themselves are less strain sensitive if not fully reacted. Besides the thermal contraction during the cooling from about 1000 K to 4 K axial stress is applied to the conductor by several manners. The force used for winding a magnet is giving tension, while the bending force gives rise to tensile and compressive strain above or below the neutral wire axis. In the finished magnet, the Lorentz force $F = J \times B$ leads to hoop stresses, related to the radius of the winding. Therefore, $\sigma = J \times B \times r$, where r is the radius, leads to very large forces, which makes special reinforcement measures necessary in the magnet or the winding package.

At the stress-compensated state, ϵ_m, the upper magnetic flux density B^*_{c2}, which is strain dependent but always below

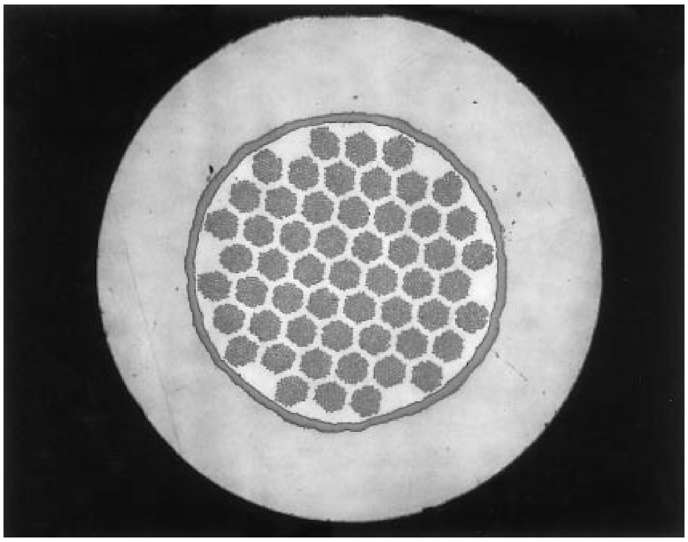

(a)

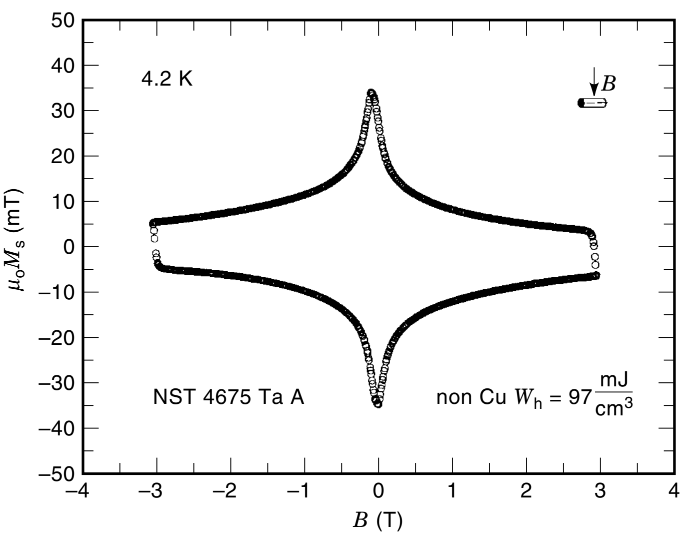

(b)

Figure 14. (a) Cross section of an ITER conductor for the central solenoid (HP II specification, i.e., low loss) with a Cu to non-Cu ratio of 1.5 and 4675 (Nb, Ta) filaments. (courtesy of Vacuumschmelze); (b) Magnetization curve of the conductor shown in Fig. 14(a), indicating the low hysteresis losses of 97 mJ/cm³ (measurements: Vacuum schmelze).

B_{c2}, can be calculated from the measured I_c by using Kramer's law (41).

At ϵ_m, the axial strain of the conductor at which $I_{c,max}$ is reached is in the range of 0.3% to 0.7%, leading to intrinsic strain $\epsilon_0 = \epsilon - \epsilon_m$. The maximum critical current is not correlated to the magnetic field. Nevertheless, the difference of I_c at ϵ and I_c at ϵ_m strongly depends on the applied magnetic field. At 12 T, between the compressive states ϵ and ϵ_m, the difference in I_c is about 20% and at 16 T there is a factor of about 2. The detailed effects of intrinsic strain on the critical magnetic field B_{c2} and the critical current density J_c can be seen in Fig. 16 and Fig. 17. The influence of the other conductor components besides the filaments and the bronze, like stabilizers or diffusion barriers is, of course, not negligible. A description of I_c/I_{cm} concerning the dependency on both magnetic field and strain, is given by the strain scaling law (42):

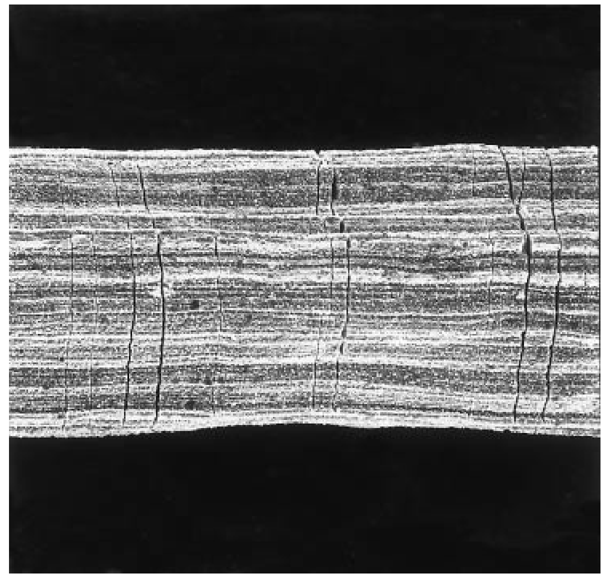

Figure 15. Scanning electron microscope micrograph showing Nb_3Sn layers after strain of the conductor of 3% (courtesy Vacuumschmelze).

$$\frac{I_c}{I_{cm}} = \left[\frac{B^*_{c2}(\epsilon)}{B^*_{c2m}}\right]^{n-p}\left[\frac{1 - B/B^*_{c2}(\epsilon)}{1 * B/B^*_{c2m}}\right]^{q}$$

In this formula n, p, and q are scaling parameters, which can be found together with the values of B^*_{c2m} for Nb_3Sn and V_3Ga in Table 5.

The mechanical behavior of V_3Ga depends mainly on the volume portion of V, while an increase of the Ga concentration reduces the tolerance with respect to mechanical loads. Conductors fabricated by the in situ technology show considerably higher mechanical values than filamentary bronze pro-

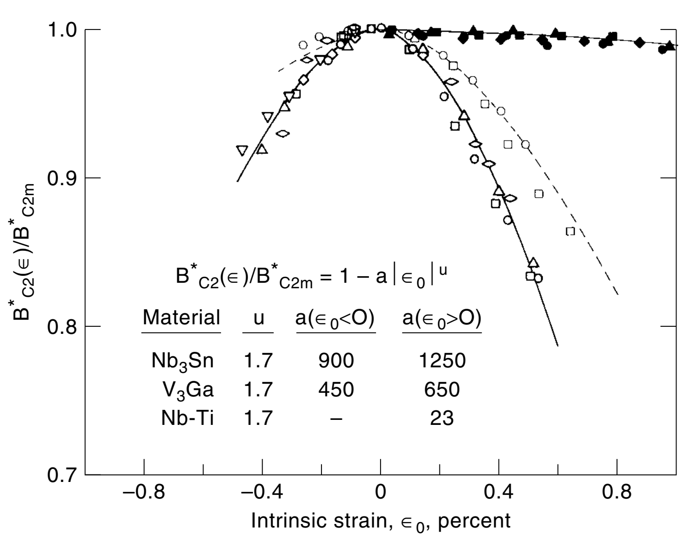

Figure 16. Upper critical field B^*_{c2} as a function of intrinsic strain ϵ_0 (42).

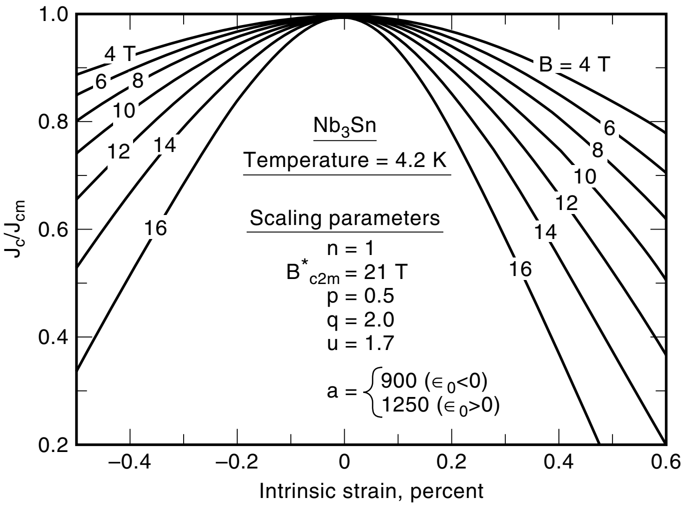

Figure 17. Relative critical current density J_c/J_{cm} as a function of intrinsic strain ϵ_0 for different magnetic fields (42).

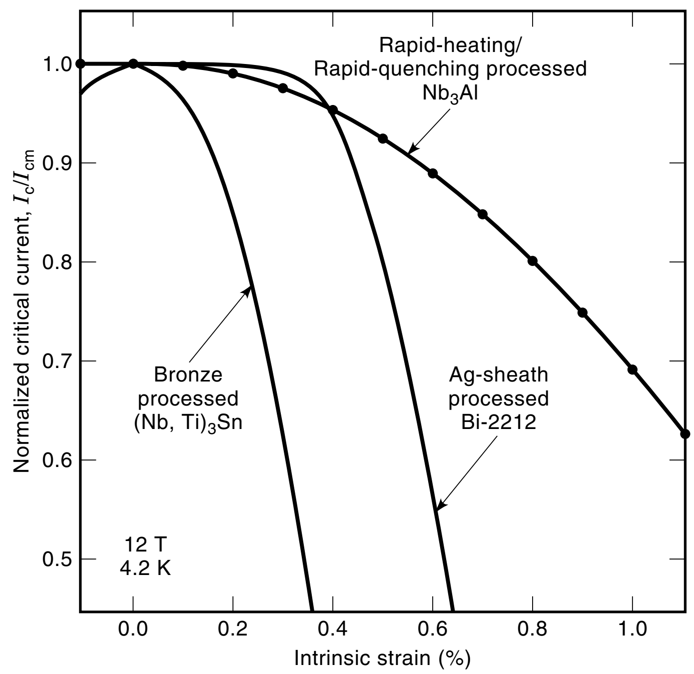

Figure 18. Critical current I_c versus intrinsic strain ϵ_0 for bronze-processed $(Nb, Ti)_3Sn$ wire, and a new Nb_3Al wire processed by rapid-heating/rapid-quenching. The strain sensitivity of the Nb_3Al compared with the $(Nb, Ti)_3Sn$ (30).

cess conductors (43). There is not a clear $I_{c,max}$, but degradation is also smaller or completely recovered, respectively, after the load has been released.

Additions of third elements influence the I_c, B_{c2}, and T_c values. Effects of strain can be seen as a function of B or B_{c2}. Due to the increase of B_{c2} by addition of Ti, Hf, or Ta to the matrix or to the core material, the effect of strain on B_{c2} is reduced. Further influence is given by the growth rate of the layer and, therefore, the remaining unreacted part of the core. Wires of Nb_3Al are less strain-sensitive; even with an intrinsic strain of 0.5% I_c is reduced only by approximately 10%, as shown in Fig. 18.

The martensitic phase transition temperature T_m increases with the compressive strain, showing an influence of the cubic-to-tetragonal distortion of the lattice and the degradation of T_c and J_c (44). At the strain ϵ_m with J_c having its maximum, the Nb_3Sn phase becomes cubic again. The effect of transverse compression on I_c is similar to that of axial strain. An increase of transverse strain σ_t is leading to a small I_c enhancement. At higher σ_t, the I_c encounters a strong reduction. The sensitivity of I_c on transverse strain is higher than for axial strain and the irreversible behavior for σ_t starts at a level which is about 25% of the comparable axial strain (45). Transverse compression may occur in large magnet assemblies like Tokamaks, with each magnet having close and strong neighboring magnets. Because of the high currents necessary in such magnets, conductors are likely to be cabled and enveloped in a stainless-steel conduit. A mixture of compressive radial stresses and transverse pressures is obtained. Especially braiding procedures of the wires are leading to many crossover points with high stress concentrations. Tetragonal distortion is also caused by compression of the unit cell by radial stresses (45). Axial stresses are applied more frequently to conductors, but in view of the higher sensitivity to σ_t, the transverse compression has to be carefully taken into account for magnet engineering as well.

Table 5. Scaling Parameters for the Use with the Strain Scaling Law (42)

Material	n	p	q	B^*_{c2m}
Nb_3Sn	1	0.5	2	21
V_3Ga	1.3	0.4	1.0	21

HEAT-TREATMENT PRINCIPLES AND CONDITIONS

The enhancement of the critical properties of practical superconductors depends on improvements in the composite. It is further necessary to use production methods and diffusion treatments that are optimized toward the required features of magnets with high magnetic fields (>20 T) and high field homogeneity. Multiple, sometimes interacting measures are necessary to increase and to stabilize the values of J_c and B_{c2}. By far, not all effects in the many different A15 members are understood. Most of the information, gained by research work, is available for bronze conductors, especially for those of the Nb_3Sn system, including internal-Sn and jelly roll conductors.

The speed of the reaction of the material in the course of the heat treatment, during which the A15 phase is formed, is correlated to the quotients of the atomic radii. The characteristic diffusion speed responsible for the ordering of the A ions to form the characteristic chains, depends on the radii of the B atoms. The smaller these radii are, the faster the diffusion process may occur (46). However, stoichiometric systems call for limits in the heat treatment. To have high concentrations of B ions, the solubility and workability of the components have to be shifted toward their limits. The thickness of the A15 layers formed per unit of time can be calculated by Fick's diffusion law, applied at the interface of two diffusion layers. The theoretical prediction for the amount of A15 phase that

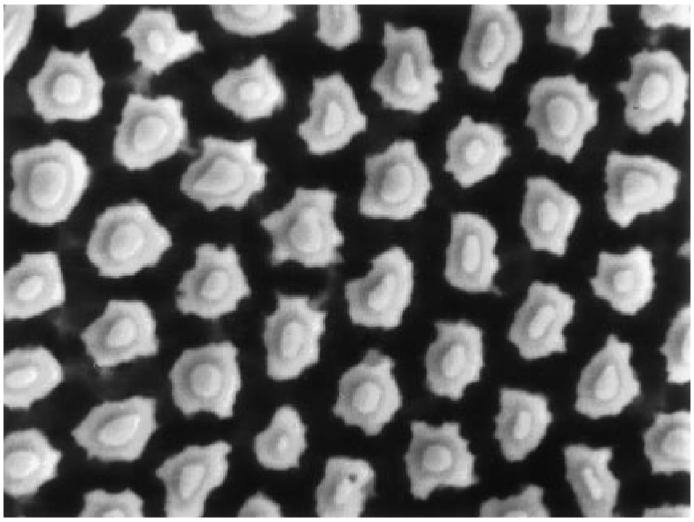

Figure 19. Layers (thickness ≈ 1 μm) of (Nb, Ta)$_3$Sn around the unreacted (Nb, Ta) core of a bronze conductor (courtesy of Vacuumschmelze).

is formed, depending of the time t, is a proportionality of $t^{0.5}$. Due to influences such as grain growth or decreasing B ion concentration during the transition process, the kinetic parameters are reduced in relation to the theoretical prediction. Measurements of the speed of layer formation in Nb_3Sn have shown proportionalities to powers of the time t in the range from 0.30 to 0.35 (32). In case where ternary or quarternary alloys are utilized, the mechanism of the diffusion process is similar, but the formation speed is influenced.

The pinning of fluxoids penetrating into type-II-superconductors needs structural imperfections. Such imperfections may be grain boundaries, lattice disturbances, grain morphology, impurities, or combinations thereof. As the coherence length ξ in Nb_3Sn is only about 3.5 nm, it is difficult to get a complete picture of the interactions which are necessary, in order to trap a fluxoid in the superconducting layers. In general, the increase of I_c depends on the heat-treatment temperature and time. Additional time and/or a higher temperature lead to a larger layer thickness. In Fig. 19, filaments with an A15 layer and an unreacted core of Nb in a bronze process conductor have been prepared so as to visualize the layer thickness of about 1 μm. Nevertheless, J_c in the layer may be decreased by grain growth, because in the intermediate field range, the maximum pinning force is related to the average grain size and the grain size distribution in the A15 layer. Thus, the critical current I_c is inversely proportional to the grain size and, therefore, proportional to the number of grain boundaries per unit volume which act as pinning center. Grain growth reduces the specific grain boundary area and diminishes the amount of fast diffusion paths. Diffusion at higher temperatures leads to faster layer formation and finer grain, but by depleting the bronze of B ions, Kirkendall voids are formed. This leads to a reduction in the diffusion rate. If those voids are located at the bronze-to-layer interface, I_c degradation may occur due to their influence on the strain behavior. Therefore, the gradient of the concentration of Sn over the cross section has to be taken into account for all heat-treatment models. It is also important to have stoichiometric conditions, that is, a Sn concentration that is sufficiently high. For jelly roll and internal-Sn composites this can be achieved to a good degree. The so-called bronze route is limited by solubility and workability reasons to about 15 wt.% Sn. It is further necessary that the bronze be uniform, especially that the variation of the Sn concentration over the cross section is small. Filament sizes and filament spacings have to be watched, to leave sufficiently wide diffusion paths and to avoid bridging of filaments, in order not to end up with large effective filament diameters d^*.

TERNARY ELEMENTS

The increase of J_c in the A15s is dominated at the intermediate field range by flux pinning at the grain boundaries. The pinning force density F_p is equal to the product of J_c and the corresponding magnetic flux density $B(F_p = J_c \times B)$. According to Kramer's law, the pinning force shows saturation in the high field region B_{c2}^*. Increasing B_{c2} leads to an increasing J_c within the A15 layer. The value of B_{c2} is dominated by the normal state resistivity ρ_0 and the critical temperature T_c. As it is not easy to increase T_c remarkably, the main means for varying B_{c2} is given by the normal state resistivity ρ_0, measured just above T_c or by the resistivity ratio. Such an increase in ρ_0 results in an increase of the Ginzburg–Landau-parameter $\kappa = \lambda/\xi$, where λ is the penetration depth (47). Because of the proportionality of the upper critical field B_{c2} to the Ginzburg–Landau parameter κ, the former is raised, too. Raising ρ_0 is possible by impurities, irregularities in the chemical composition, causing microstructural defects. B_{c2} is not depending on the grain size, but its upper limit is determined by the susceptibility according to Pauli's paramagnetic effect (43). For that reason, the flux-pinning force and the grain boundaries are not relevant if the magnetic field B is close to B_{c2}.

Besides the more principal aspects, there are different other reasons which are influencing the performance of practical A15 superconductors. Disturbances in the microstructure are originating from the production process, chemical nonhomogeneities, or variations of filament diameters over the length (sausageing). Nonuniformity of A15 layers due to nonuniform distribution and supply of B ions is strongly influenced by the conductor design. Those macroscopic effects are also observed for designs leading to irregular working and deformation conditions due to the combination of materials with quite different ductility, like Nb, Cu, and Sn. Microcracks occur in the layer itself, caused by thermal or handling defects. Bronze matrix conductors need, because of work hardening, intermediate heat treatments to preserve or to restore the ductility. Prereaction to a substantial degree may be encountered. It leads to heterogeneous deforming conditions, reduction of the Sn supply for the final diffusion treatment, and mechanical defects in the conductors. Therefore, intermediate heat-treatment temperatures must be chosen carefully and should not exceed 500°C. Additionally, time has to be restricted.

To achieve better properties of A15 conductors, doping with defined impurities like Zn, Mg, Fe, and Ni, and also alloying with higher contents of Ti, Ta, or Ga has been performed. The stoichiometry in a ternary or a quartenary compound is a rather demanding field. The variety of metallurgical treatments like alloying, in combination with numbers of

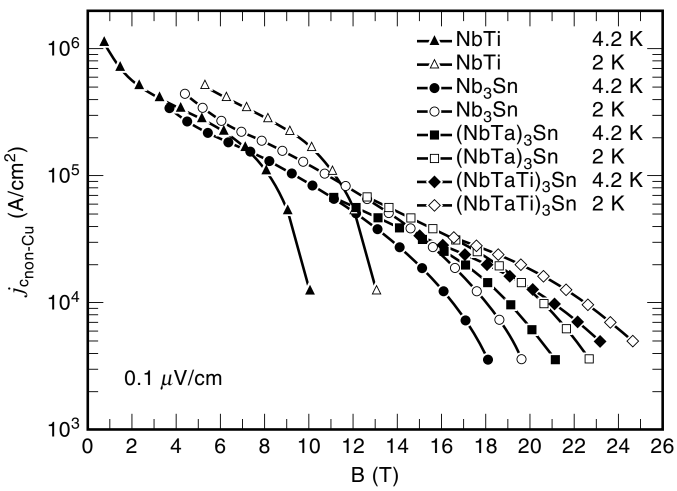

Figure 20. Non-Cu critical current density J_c versus magnetic field for Nb_3Sn (undoped, doped with Ta, or Ta and Ti, respectively) at temperatures of 4.2 K and 2 K (measurement: Vacuumschmelze).

different heat treatments, result in remarkable effects. Some of the additives, for example, in the bronze matrix, are influencing the diffusion process like speed and grain refinement, which enhances the performance of conductors in the intermediate field region. Others are more effective by increasing J_c at high fields due to an increase of B_{c2}. There is not a complete correlation given between composites and increase of J_c for the entire field range. This is not surprising at all, since additives may be deposited at the grain boundaries. Therefore, crossover of J_c versus B for doped or undoped conductors or for conductors doped with different additives is observed, as shown in Fig. 20.

The different atomic radii of the additives in relation to the basic alloy is also of influence. Ti with a smaller atomic radius is incorporated more completely into the Nb lattice than zirconium (Zr) or hafnium (Hf) with larger atomic radii. The embedding of the Ti, originating from the matrix Cu-Sn into Nb_3Sn, is at a larger degree than for the Ti alloyed with the Nb core. Elements like Ti, Zr, and Hf for alloying Nb result in A15 layers with fine grains. Mg in bronze, like Cu-Sn or Cu-Ga, is increasing the formation rate of the A15 phase, which causes grain refinement. The low T_c of V_3Ge can be raised from 6 K to about 10 K by adding 8 at.% Al (43). Ti in Nb cores (about 2 at.%) is increasing the layer thickness. The improvement of J_c in Nb_3Sn by alloying Hf to the core and additional Ga to the matrix is remarkable and leads also to an increase of the irreversible strain ϵ_d (43), but especially alloying with Ga is difficult and impractical. V_3Ga, which has already superior high field values, improves further above 20 T, when adding Ga to the V core and Mg to the Cu-Ga matrix. As Ti speeds up the diffusion rate of Sn in Nb, a doping with 0.3 wt.% Ti, in combination with high-Sn-bronze (15 wt.%) shows improved values of non-Cu J_c (33), see Fig. 10. By introducing Ge into the matrix of a Nb_3Sn composite, the thickness of the A15 layer is reduced significantly. This is most probably related to the formation of an additional phase with the Ge (Nb_6Ge_5) at the interface between core and matrix (22). The grain size, however, is smaller, and so J_c in the layer is enhanced.

The heat-treatment time and temperature is in interaction with additional elements, or combinations thereof, responsible for the formation of the A15 layer. For wind-and-react technology, it is indispensable to limit the temperature, due to the insulation materials available. Practical glass-braid insulations for temperatures of up to 700°C and 800°C, respectively, are at hand. The temperature–time combination is further determined by the application of conductors. Additions of Ta, for example, Nb 7.5 wt.% Ta, reduces the formation rate of the A15 phase (48), but increases J_c due to a longer heat treatment. In the case of intermediate magnetic fields, filament diameters should be smaller, leading, even with Ta doping, to a relatively short heat-treatment time, to realize, in this range of magnetic field, the required fine grain. Especially for conductors which are to be used at higher fields, the

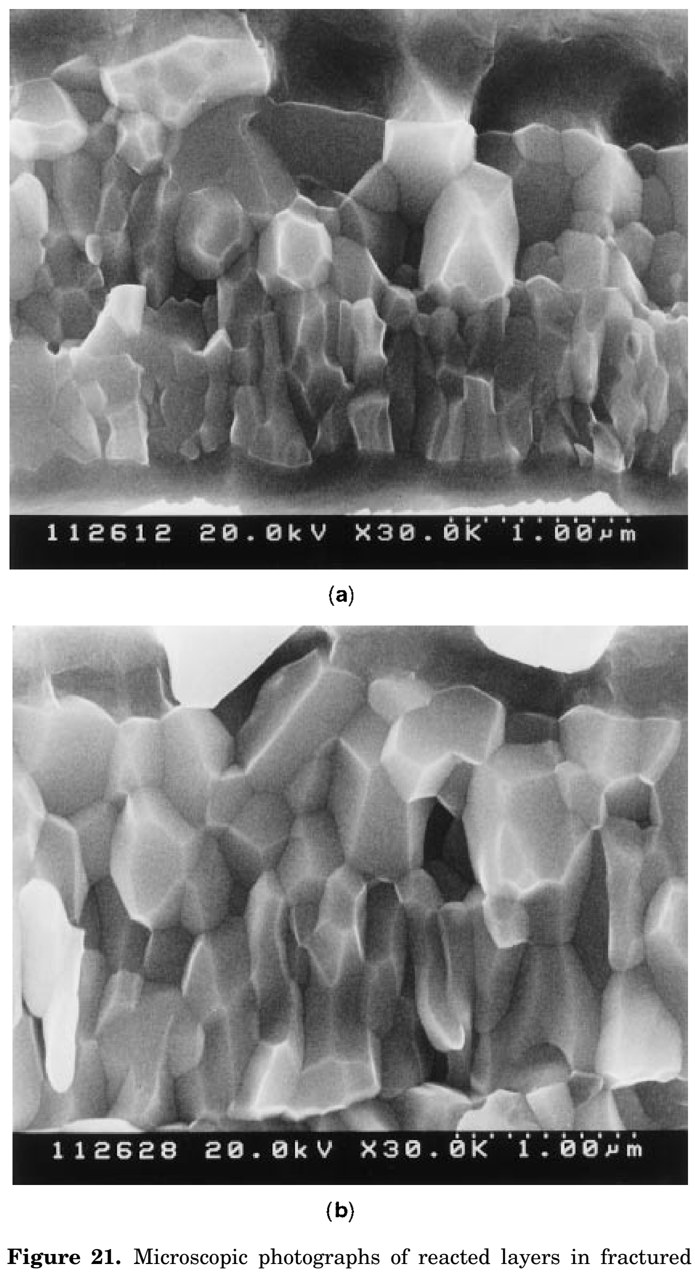

(a)

(b)

Figure 21. Microscopic photographs of reacted layers in fractured cross sections of samples heat treated at (a) 700°C for 100 h; and (b) 750°C for 150 h (courtesy of Kobe Steel).

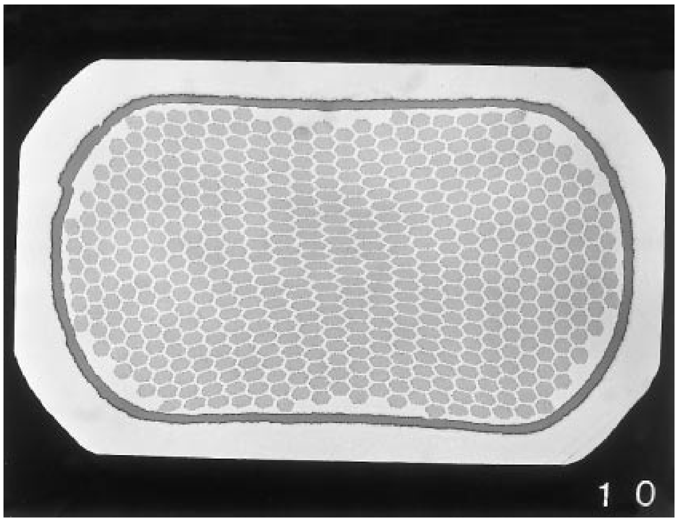

Figure 22. Externally stabilized (Nb, Ta)$_3$Sn conductor with a Ta diffusion barrier and outer Cu stabilization for high-resolution NMR magnets (courtesy of Vacuumschmelze).

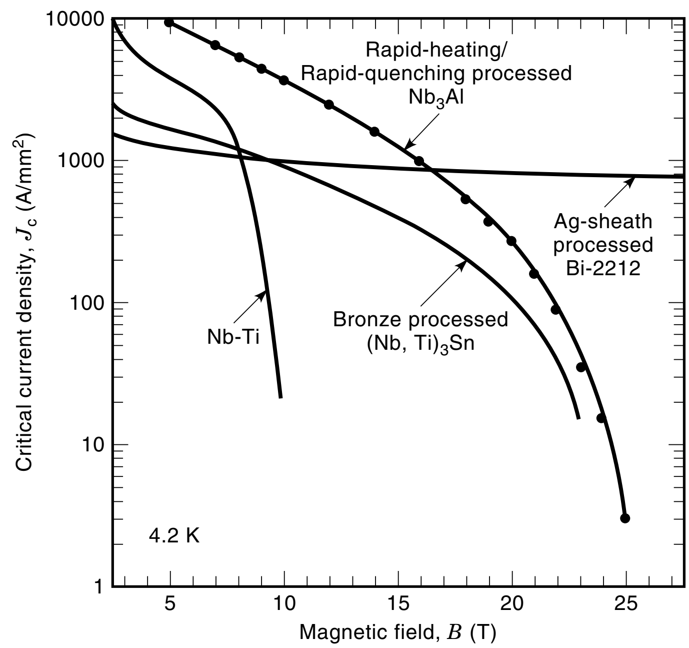

Figure 23. Non-Cu critical current density J_c versus magnetic field B for a bronze-processed (Nb, Ti)$_3$Sn and a Nb_3Al rapid-heating/rapid-quenching processed wire at a temperature of 4.2 K (30).

filament diameters are increased, as well as heat-treatment time and temperature. Often, more than one different cycle is executed, to improve the formation of the A15 layer, as not too much attention should be paid to grain growth, in view of the high field application. It is furthermore understood that, for each grain size, pinning interaction may be different, and flux line–lattice spacing is reason for different numbers of flux lines in each grain (49). The variability of the grain sizes for different heat treatments, but also within one sample, becomes evident in looking at the microscopic photographs in Fig. 21(a) and Fig. 21(b).

The necessity to fulfill the requirements of high critical currents I_c at high magnetic fields B_{c2} leads automatically to large conductor cross-sections with a high number of filaments. Therefore, more than 100,000 filaments and cross-section areas of more than 6 mm^2 are unavoidable. Figure 22 is an example of such an externally stabilized Nb_3Sn conductor. For several years, the demand for high magnetic fields and magnets with larger bores has been the driving force in the development of A15 superconductors. While the first successful magnets were built from tape conductors (13), round or rectangular wires became the more favorable solutions.

For magnetic field strengths of above 9 T in the center of the magnet, materials with high B_{c2}, like conductors with A15 structure, are necessary. The study of polymers or macromolecules demands NMR systems of up to 1 GHz proton-resonance frequency (Larmor frequency); this corresponds to a magnetic field of 23.5 T. Thus all NMR systems working at frequencies of more than 400 MHz (corresponding to a magnetic field of 9.4 T) need other conductor material than NbTi. At a temperature of 2 K and a field of up to 21 T, Nb_3Sn still shows reasonable I_c values. Other composites, like the rapid-quenched Nb_3Al, may perform even better according to Fig. 23. Besides the NMR applications, which are dominated by bronze route conductors, diffusion technology is substantial for conductors that are subject to a high magnetic field. For big machines like ITER, more than 1,000 tons of A15 conductors will be necessary.

Laboratory scale solenoids with magnetic fields of up to 20 T or high field split coils take advantages of the improved current densities J_c of, for example, internal-Sn, modified jelly roll, or tube-processed wires. Special dipole and quadrupole magnets for accelerators have to reach magnetic fields of more than 11 T, which is only achievable with A15 conductors like the internal Sn type shown in Fig. 24. Hybrid magnet systems, made of a combination of superconductive and resistive magnets, are capable of reaching fields of up to 45 T or 50 T. Not only the high critical fields B_{c2}, but also the superior values of the critical temperature T_{c2}, are further advantages of these materials, which can even be used, with refrigerator cooling, for magnetic fields of 5 T to 10 T. Tapes of Nb_3Sn with a Nb-1% Zr-core are used to build split-coils acting as open MRI systems, operating at 9 K (16).

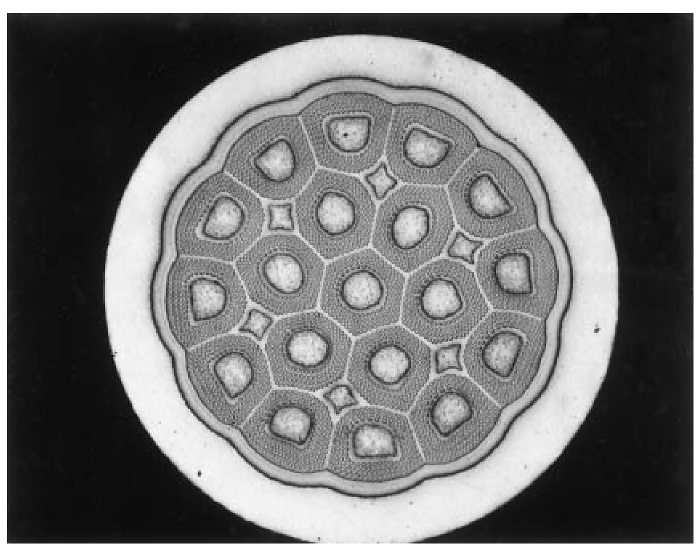

Figure 24. Cross section of an internal tin conductor for use in high-field dipole magnets (courtesy IGC).

The results showing the improvements of the properties of A15 superconductors have been obtained, to a considerable degree, on an empirical basis. To force this technology forward, even more empirical work will be necessary. Fundamental tasks, like improvement of the composite, layer homogeneity, and grain morphology, will be inevitable for controlling the microstructural influences in future designs. Introducing artificial pinning centers (APC) and their possible variations and controlled grain refinement will be another route to be followed.

BIBLIOGRAPHY

1. H. Hartmann et al., *Z. Anorg. Chem.* **198**: 116, 1931.
2. M. Weger and I. B. Goldberg, Some lattice and electronic properties of the β-tungstens, *Solid State Phys.,* **28**.
3. W. Buckel, *Supraleitung,* Weinheim, Germany: VCH, 1984.
4. J. Muller, A15 type superconductors, *Rep. Proc. Phys.,* **43**: 1980.
5. G. F. Hardy and J. D. Hulm, *Phys. Rev.,* **87**: 884, 1953.
6. B. T. Matthias et al., *Phys. Rev.* **95**: 1435, 1954.
7. W. Klose, *Sommerschule für Supraleitung,* Pegnitz, Germany: DPG, 1970, p. 14.
8. O. Henkel et al., *Supraleitende Werkstoffe,* Leipzig, Germany: VEB Verlag für Grundstoffindustrie, 1982.
9. J. Bardeen, L. N. Cooper, and J. R. Schrieffer, Theory of superconductivity, *Phys. Rev.,* **108**: 1175, 1975.
10. B. W. Batterman and C. S. Barrett, *Phys. Rev.,* **13**: 390, 1964.
11. H. J. Williams and R. C. Sherwood, *Bull. Amer. Phys. Soc.* **5**: 430, 1960.
12. British patent, GB.No.1203292, 1966.
13. W. D. Markiewicz et al., A 17.5 T superconducting concentric Nb3Sn and V3Ga magnet system, *IEEE Trans. Magn.* **MAG-13**: 35, 1977.
14. K. Tachikawa and Y. Tanaka, *Japan. J. Appl. Phys.* **5**: 834, 1966.
15. E. W. Collings, Processing of Nb_3Al superconductors, Rep., Columbus, OH: Ohio State University, 1997.
16. C. G. King et al., Flux jump stability in Nb_3Sn tape, *IEEE Trans. Appl. Supercond.,* **7**: 1524–1528, 1997.
17. E. W. Collings, Recent advances in multifilamentary Nb_3Al strand processing, Rep., Columbus, OH: Ohio State University, 1997.
18. J. F. Kunzler et al., *Phys. Rev. Lett.,* **6**: 89, 1961.
19. M. R. Pickus et al., *Filamentary A15 Superconductors,* New York: Plenum, 1980, p. 331.
20. BMFT, *Entwicklung von Hochfeldsupraleitern,* BMFT-FB T, 1976.
21. D. Larballestier et al., Rutherford Lab. Report 74-135, *IEEE Trans. Magn.* **MAG-11**: 247, 1970.
22. T. Pyon and E. Gregory, Some effects of matrix additions to internal tin processed multifilamentary Nb_3Sn superconductors, *IEEE Trans. Appl. Supercond.,* **5**: 1760–1763, 1995.
23. M. Hansen, *Constitution of Binary Alloys,* New York: McGraw-Hill, 1958, p. 634.
24. E. Gregory et al., Development of Nb_3Sn wires made by the internal tin process, CEC/ICMC, AB-6, 1997.

25a. Y. Ikeno et al., Development of Nb_3Sn superconducting wire using an in-situ processed large ingot, in *Advances in Cryogenic Engineering,* vol. 36a, New York: Plenum, 1990.

25b. H. Fuji et al., Development of react and wind coils using in-situ Nb_3Sn wires for ac applications, MT15, 1997.

26. S. Ceresara et al., *IEEE Trans. Magn.* **MAG-15**: 639, 1979.
27. W. K. McDonald, *Expanded metal containing wires and filaments,* US patent 4414428, 1983.
28. R. G. Sharma, Multifilamentary V3Ga wires and tapes with composite covers, *Cryogenics,* **25**: 381, 1985.
29. J. L. Jorda and R. Flückiger, Département de Physique de la Matiére Condensée, Genéve, *J. Less-Common Metals,* **75**: 227 (1980).
30. K. Inoue et al., *New Nb_3Al Multifilamentary Conductor and Its Application to High-Field Superconducting Magnets,* Tsukuba-Shi, Ibarak: 305, Japan: RHMF, 1997.
31. K. Tachikawa, *Proc. ICEC,* **3**, 1970.
32. H. Hillmann, Fabrication technology of superconducting material, *Superconductor Material Science,* New York: Plenum, 1981.
33. T. Miyazaki et al., Improvement of critical current density in the bronze processed Nb_3Sn superconductor, Paper CPB-7, CEC/ICMC, 1997.
34. H. Krauth et al., *Int. Workshop on High Magn. Fields,* 1996.
35. Y. Miyazaki et al., Development of bronze processed Nb_3Sn superconductors for 1 GHz NMR magnets, Paper CPB-6, CEC/ICMC, 1997.
36. M. Thöner et al., Aluminum stabilized Nb_3Sn superconductors, *Adv. Cryog. Eng.,* **34**: 507, 1987.
37. E. Wang et al., Evaluation of Nb_3Sn superconductors for use in a 23.5 T NMR magnet, *IEEE Trans. Magn.,* **30**: 2344–2347, 1994.
38. H. G. Knoopers et al., Third round of the ITER strand benchmark test, EUCAS conference applied superconductivity, no. 158, IOP conference series, 1997.
39. E. Buehler and H. J. Levingstein, *J. Appl. Phys.,* **36**: 3856, 1965.
40. G. Rupp, The importance of being prestressed, in M. Suenaga and A. F. Clark, eds., *Filamentary A15 Superconductors,* New York: Plenum, 1980.
41. E. J. Kramer, *J. Appl. Phys.,* **44**: 1360, 1973.
42. J. W. Ekin, Stress/strain effects on critical current, *Cryogenics,* **35**: S25–S28, 1995.
43. K. Tachikawa, Recent developments in filamentary compound superconductors, *Adv. Cryog. Eng.,* **28**: 1982.
44. R. W. Hoard et al., The effect of strain on the martensitic phase transition in superconducting Nb_3Sn, *IEEE Trans. Magn.,* **MAG-17**, 1981.
45. W. Specking et al., Effect of transverse compression on I_c of Nb_3Sn multifilamentary wire, *Adv. Cryog. Eng.,* **34**: 569, 1988.
46. T. Luhmann and A. R. Sweedler, *Phys. Lett.,* **58A**: 355, 1976.
47. V. I. Ginzburg and L. L. Landau, *Žurn. Ekspr. Teor. Fyz.,* **20**: 1064, 1950.
48. W. Specking, F. Weiss, and R. Flukiger, Effect of filament diameter and spacing on J_c of Nb3Sn wires in the intermediate filed range and at high fields, *IEEE Trans. Magn.,* **23**: 1188–1191, 1987.
49. D. Rodrigues, Jr. et al., Flux pinning mechanisms in superconducting A15 materials and the optimization of their transport properties, to be published in *Adv. Cryog. Eng.,* **44**: 1998.

REINHARD DIETRICH
Vacuumschmelze GmbH